Studies of Structure and Phase Transition in $[C(NH_2)_3]HgBr_3$ and $[C(NH_2)_3]HgI_3$ by Means of Halogen NQR, ^1H NMR, and Single Crystal X-Ray Diffraction

Hiromitsu Terao, Masao Hashimoto[a], Shinichi Hashimoto[a], and Yoshihiro Furukawa[b]

Department of Chemistry, Faculty of Integrated Arts and Sciences, Tokushima University, Minamijosanjima-cho, Tokushima 770-8502, Japan

[a] Department of Chemistry, Faculty of Science, Kobe University, Nadaku, Kobe 657-8501, Japan

[b] Faculty of School Education, Hiroshima University, Kagamiyama, Higashi-Hiroshima 739-8524, Japan

Reprint requests to Dr. H. T.; E-mail: terao@ias.tokushima-u.ac.jp

Z. Naturforsch. **55 a,** 230–236 (2000); received August 23, 1999

Presented at the XVth International Symposium on Nuclear Quadrupole Interactions, Leipzig, Germany, July 25 - 30, 1999.

The crystal structure of $[C(NH_2)_3]HgBr_3$ was determined at room temperature: monoclinic, space group C2/c, $Z = 4$, $a = 775.0(2)$, $b = 1564.6(2)$, $c = 772.7(2)$ pm, $\beta = 109.12(2)°$. In the crystal, almost planar $HgBr_3^-$ ions are connected via Hg···Br bonds, resulting in single chains of trigonal bipyramidal $HgBr_5$ units which run along the c direction. $[C(NH_2)_3]HgI_3$ was found to be isomorphous with the bromide at room temperature. The temperature dependence of the halogen NQR frequencies ($77 < T/K <$ ca. 380) and the DTA measurements evidenced no phase transition for the bromide, but a second-order phase transition at (251 ± 1) K (T_{c1}) and a first-order one at (210 ± 1) K (T_{c2}) for the iodide. The transitions at T_{c2} are accompanied with strong supercooling and significant superheating. The room temperature phase (RTP) and the intermediate temperature phase (ITP) of the iodide are characterized by two $^{127}I_{(m=1/2\leftrightarrow3/2)}$ NQR lines which are assigned to the terminal and the bridging I atoms, respectively. There exist three lines in the lowest temperature phase (LTP), indicating that the resonance line of the bridging atom splits into two. The signal intensities of the $^{127}I_{(m=1/2\leftrightarrow3/2)}$ NQR lines in the LTP decrease with decreasing temperature resulting in no detection below ca. 100 K. The $^{127}I_{(m=1/2\leftrightarrow3/2)}$ NQR frequency vs. temperature curves are continuous at T_{c1}, but they are unusual in the LTP. The T_1 vs. T curves of ^1H NMR for the bromide and iodide are explainable by the reorientational motions of the cations about their pseudo three-fold axes. The estimated activation energies of the motions are 35.0 kJ/mol for the bromide, and 24.1, 30.1, and 23.0 kJ/mol for the RTP, ITP, and LTP of the iodide, respectively.

Key words: $[C(NH_2)_3]HgX_3$; Crystal Structure; Phase Transition; NQR; ^1H NMR.

Introduction

Compounds with the formula $RHgX_3$, R_2HgX_4, RHg_2X_5 (R = alkylammonium, X = Cl, Br, I) are formed between mercury(II) halides and alkylammonium halides. They show a wide variety of structures depending not only on the size and symmetry of the cations, but also on the electrostatic interactions and the hydrogen bonding (H-bond) between the cat- and anions. Generally discrete $HgBr_4^{2-}$ tetrahedra exist in R_2HgX_4, whereas one-dimensional anion chains are usual in $RHgX_3$ and RHg_2X_5 (See e. g. [1, 2]). The crystals exhibit quite frequently phase transitions associated with disorder of the cations. Phase transitions are found more often for the compounds with smaller cations than for those with larger ones [3].

In addition to the size of the cations, the character of the N-H···X hydrogen bonds between cations and anions are related to the appearance of phase transitions, because the H-bonds restrict the thermal motion of cations. Then the number of NH_x ($x = 1 \sim 3$) groups, i.e. the number of H-bonds per cation seems an important factor controlling the phase transitions. From this point of view the guanidinium ion $[C(NH_2)_3]^+$

0932–0784 / 00 / 0100–0230 $ 06.00

Table 1. Experimental conditions for the crystal structure determination and crystallographic data of $[C(NH_2)_3]HgBr_3$.

Formula	$CH_6Br_3HgN_3$
Formula weight	500.38
Crystal habit	Needle (colorless)
Size/$(mm)^3$	$0.05\times0.05\times0.20$
Temperature/K	298
Absorption coeff. (μ/m^{-1})	30936
Diffractometer	Rigaku AFC5R
Wavelength/pm	71.07 (MoK_α)
Monochromator	Graphite (002)
Scan	$\omega/2\theta$
$(\sin\theta/\lambda)_{max}/pm^{-1}$	0.006496
Reflections measured	1129
Symmetry independent	1054
Considered $F_0 > 3\sigma(F)_0$	614
Number of free parameters	52
$F(000)$	872.00
$R(F)$	0.030
$R_w(F)$	0.011
Lattice constants a/pm	775.0(2)
b/pm	1564.6(2)
c/pm	772.7(2)
β/°	109.12(2)
$V_{ucell}\times10^{-6}/(pm)^3$	885.3(4)
Space group#	C_{2h}^6 - C2/c
Formula units/Unit cell (Z)	4
$\rho_{calc}/Mg\cdot m^{-3}$	3.754
$\rho_{obs}/Mg\cdot m^{-3}$	3.75

Point positions: x, y, z; $-x, y, \frac{1}{2}-z$; $-x, -y, -z$; $x, -y, \frac{1}{2}+z$; $\frac{1}{2}+x, \frac{1}{2}+y, z$; $\frac{1}{2}-x, \frac{1}{2}+y, \frac{1}{2}-z$; $\frac{1}{2}-x, \frac{1}{2}-y, -z$; $\frac{1}{2}+x, \frac{1}{2}-y, \frac{1}{2}+z$.

is notable owing to its multi H-bond-forming ability. The crystal structure of $[C(NH_2)_3]CdBr_3$ has been solved by Krishnan et al. [4]. In this crystal, characteristic one-dimensional anion chains exist in which $CdBr_3^-$ units are connected by Cd···Br bonds. The ^{81}Br NQR of the cadmium compound showed no phase transition in the range $77 < T/K < 390$ [4]. In this work, we prepared $[C(NH_2)_3]HgBr_3$ and $[C(NH_2)_3]HgI_3$ for the first time and investigated their structures, bondings, and phase transitions by means of halogen NQR, ^1H NMR, single crystal X-ray diffraction, and DTA.

Experimental

The crystals of $[C(NH_2)_3]HgBr_3$ were obtained by concentrating a methyl alcohol solution containing $HgBr_2$ and $[C(NH_2)_3]Br$ in 1:1 molar ratio, and the crystals of $[C(NH_2)_3]HgI_3$ from a solution of HgI_2 and $[C(NH_2)_3]I$. $[C(NH_2)_3]Br$ and $[C(NH_2)_3]I$ were prepared by adding a stoichiometric amounts of hydrobromic acid or hydroiodic acid to $[C(NH_2)_3]_2CO_3$ dissolved in water. The C, H, and N analyses were consistent with the chemical formula; found/calc.; weight %: C: 2.46/2.40; H: 1.16/1.21; N: 8.45/8.40 for $[C(NH_2)_3]HgBr_3$ and C: 1.88/1.87; H: 0.87/0.94; N: 6.58/6.55 for $[C(NH_2)_3]HgI_3$.

Table 2. Positional and thermal parameters $B_{eq}/B^*_{iso}/(pm)^2$ in the crystal structure of $[C(NH_2)_3]HgBr_3$. Estimated standard errors in parentheses.

Atom	x/a	y/b	Z/c	$B_{eq}/B^*_{iso}\times10^{-4}$
Hg	0.5000	0.04861(3)	0.2500	4.53(2)
Br(1)	0.5000	0.20904(6)	0.2500	4.41(3)
Br(2)	0.73785 (8)	–0.04371 (5)	0.17043(8)	3.18(2)
N(1)	–0.007(1)	0.1465(4)	0.1016 (9)	5.4(2)
N(2)	0.0000	0.2722(5)	0.2500	7.3(4)
C	0.0000	0.1887(7)	0.2500	3.9(3)
H(1)	–0.053(9)	0.094(3)	0.086(9)	5.9(6)*
H(2)	0.02(1)	0.174(4)	0.03(1)	8.0(4)*
H(3)	0.03(1)	0.299(5)	0.14 (1)	13.2(4)*

The DTA measurement was carried out by using a home-made DTA apparatus.

Details of the single crystal X-ray experiment on $[C(NH_2)_3]HgBr_3$ are summarized in Table 1. The structure was solved by the direct method [5] and refined by the full matrix least squares method [6]. Non-hydrogen and hydrogen atoms were refined with anisotropic and isotropic thermal factors, respectively. A preliminary single crystal X-ray investigation on $[C(NH_2)_3]HgI_3$ showed that it is isomorphous with the bromide: monoclinic, space group C2/c, $Z = 4$, $a = 842.4(6)$, $b = 1609.6(6)$, $c = 833.5(7)$ pm, $\beta = 109\ (1)°$.

The NQR spectra obtained with a super-regenerative spectrometer. The signals were recorded on a recorder through a lock-in amplifier with Zeeman modulation. The accuracy of the frequency measurement is estimated to be within ± 0.02 MHz.

Spin-lattice relaxation times T_1 of ^1H NMR were measured by the inversion recovery method on a standard pulsed NMR spectrometer.

Results

The Crystal Structure of $[C(NH_2)_3]HgBr_3$ at Room Temperature

In Table 2 are listed the atomic coordinates and the thermal parameters. The Hg, Br(1), and N(2) atoms are located on the two-fold axis. Figure 1 shows the crystal structure and the numbering scheme for the atoms. In Table 3 are listed bond lengths and bond

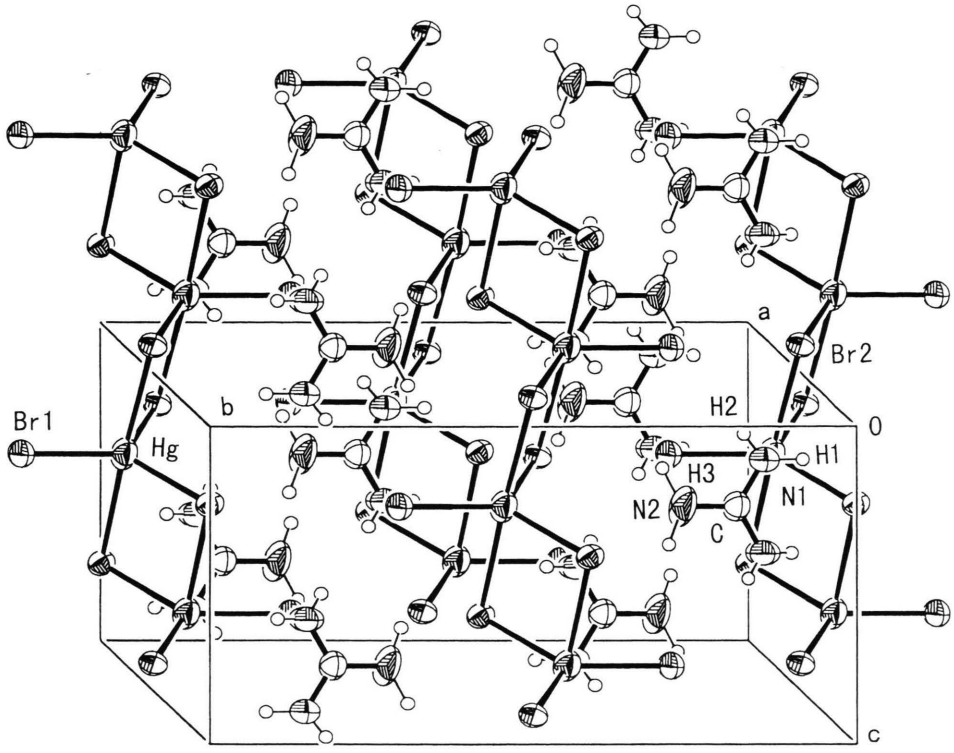

Fig. 1. The crystal structure of $[C(NH_2)_3]HgBr_3$.

Table 3. Atomic distances and angles in the structure of $[C(NH_2)_3]HgBr_3$.

Connection	*d*/pm	Connection	Angle/°
Hg-Br(1)	251.0(1)	Br(1)-Hg-Br(2)	124.20(2)
Hg-Br(2)	257.0(1)	Br(1)-Hg-Br(2′)	91.39(2)
Hg-Br(2′)	316.8(1)	Br(2)-Hg-Br(2′)	90.55(3)
C-N(1)	130.8(8)	Br(2)-Hg-Br(2″)	111.61(4)
C-N(2)	131(1)	Br(2)-Hg-Br(2‴)	87.89(3)
		Br(2′)-Hg-Br(2‴)	177.22(4)
		Hg-Br(2)-Hg	92.11(3)
Br(1)···N(1)	354.9(7)	N(1)-C-N(1′)	119(1)
Br(2)···N(2)	357.9(8)	N(1)-C-N(2)	120.3(5)

Br(2′): $x, -y, \frac{1}{2}+z$; Br(2″): $1-x, y, \frac{1}{2}-z$; Br(2‴): $1-x, -y, -z$.

Table 4. ^{81}Br and $^{127}I_{(m=1/2\leftrightarrow3/2)}$ NQR frequencies (ν) of $[C(NH_2)_3]HgBr_3$ and $[C(NH_2)_3]HgI_3$.

Compound	Nucleus	Phase	*T*/K	ν/MHz		
$[C(NH_2)_3]HgBr_3$	^{81}Br		77	112.40	88.31	
			298	108.41	86.17	
$[C(NH_2)_3]HgI_3$	^{127}I	LTP	140	135.96	128.38	114.60
			210	133.63	125.52	113.60
		ITP	210	136.18	127.80	
			235	136.15	124.38	
		RTP	298	134.19	118.13	

angles for the ions together with selected N···Br contacts. Approximately planar $HgBr_3^-$ ions are interconnected via Hg···Br short contacts to result in a chain structure. The final refinement gave $R = 0.030$ and $R_w = 0.011$. The structure is isostructural with that of $[C(NH_2)_3]CdBr_3$ [4].

Bromine and Iodine NQR Spectra

The ^{81}Br and $^{127}I_{(m=1/2\leftrightarrow3/2)}$ NQR frequencies of $[C(NH_2)_3]HgBr_3$ and $[C(NH_2)_3]HgI_3$ at represen-

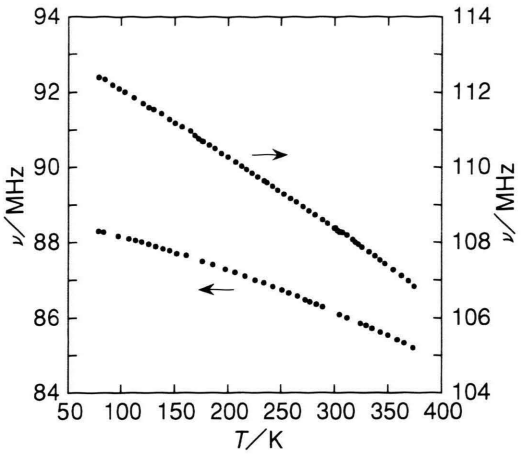

Fig. 2. Temperature dependence of ^{81}Br NQR frequencies of $[C(NH_2)_3]HgBr_3$.

tative temperatures are listed in Table 4. The assignments of bromine resonance lines to ^{81}Br were confirmed by the observation of the corresponding ^{79}Br lines. On the other hand, without the detection of resonance lines due to the $m = \pm 3/2 \leftrightarrow \pm 5/2$ transitions, the observed iodine resonance lines are safely assigned to the $m = \pm 1/2 \leftrightarrow \pm 3/2$ transitions by referring to those in $CH_3NH_3HgI_3$ [7]. The temperature dependence curves of ^{81}Br NQR frequencies of the bromide are shown in Figure 2. The lower-frequency line ν_2 is almost twice as intense as the higher-frequency line ν_1. By considering their frequencies and intensities, ν_1 and ν_2 are assigned to the terminal and the bridging Br atoms, respectively. Both ν_1 and ν_2 exhibit a normal negative temperature dependence without showing the occurrence of any phase transition.

In Fig. 3, the temperature dependence curves of $^{127}I_{(m=1/2\leftrightarrow 3/2)}$ NQR frequencies of $[C(NH_2)_3]HgI_3$ show clearly the occurrence of two phase transitions. These temperatures are determined to be T_{c1} = (251 ± 1) K and T_{c2} = (210 ± 1) K by DTA on heating, as mentioned later. The room temperature phase (RTP) gives two resonance lines ν_1 and ν_2, which are assigned unambiguously to the terminal and the bridging I atoms, respectively, by considering their frequencies and relative intensities. On cooling the RTP, ν_1 as well as ν_2 increased smoothly, but at T_{c1} they clearly changed their temperature gradients. Interestingly, in the intermediate temperature phase (ITP) below T_{c1}, the value of $d\nu_1/dT$ is almost zero or slightly negative, while the value of $d\nu_2/dT$ is negative

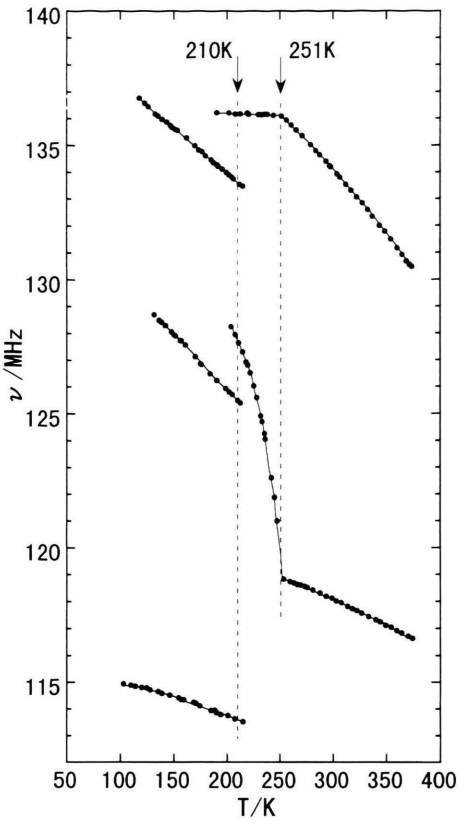

Fig. 3. Temperature dependence of $^{127}I_{(m=1/2\leftrightarrow 3/2)}$ NQR frequencies of $[C(NH_2)_3]HgI_3$.

and its magnitude is extremely large. Furthermore, on cooling, these lines of the ITP could be observed down to ca. 191 K beyond T_{c2} (supercooling of the ITP by ca. 20 K from T_{c2}). In the lowest temperature phase (LTP), below T_{c2} three lines ν'_{1-3} were observed; namely ν_2 in the ITP splits into to ν'_2 and ν'_3 in the LTP. All the lines ν'_{1-3} diminished their intensities with decreasing temperatures and disappeared below ca. 100 K. It is remarkable that these LTP lines could be observed up to 217 K beyond T_{c2} (superheating of the LTP by ca. 7 K from T_{c2}).

DTA Measurement

The DTA curve of $[C(NH_2)_3]HgI_3$ was characterized by two thermal anomalies. A representative DTA curve of the iodide is shown in Figure 4. Small anomalies with long tails on the low temperature side of the peak maximum is at T_{c1} = (251 ± 1) K, were observed both on cooling and heating. Smeared peaks were always found near 190 K on cooling, suggesting

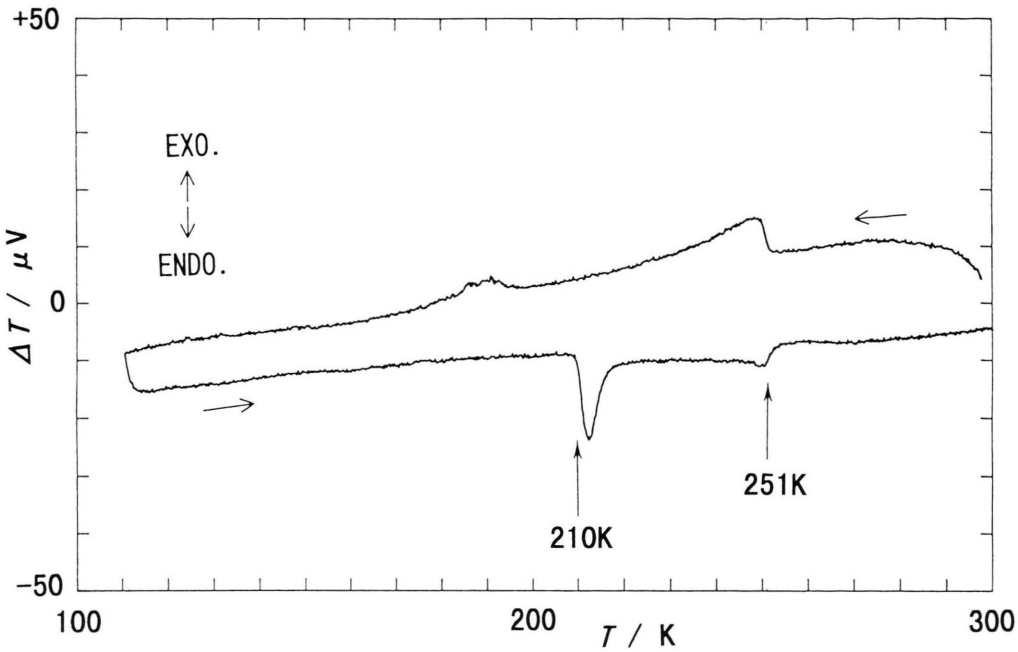

Fig. 4. The representative DTA curves observed for $[C(NH_2)_3]HgI_3$.

that the ITP→LTP transition is very slow. On heating, the LTP→ITP transition showed relatively sharp peaks, from which we deduce $T_{c2} = 210 \pm 1$ K.

Spin-lattice Relaxation Times T_1 of ^1H NMR

The temperature dependences of ^1H T_1 are given in Figure 5. For the bromide T_1 was measured at the resonance frequency 32 MHz and for the iodide at 12, 32, and 48 MHz. For the bromide, a simple V-shaped T_1 curve was observed in the log T_1 vs. $1/T$ plot, its T_1 minimum value being 27 ms at ca. 342 K. The T_1 behavior of the iodide is similar to that of the bromide but the curves are shifted toward low temperatures. At the T_{c1} transition, the T_1 values seem to be experimentally continuous on heating and cooling runs, suggesting that this transition is of second-order. At the lower T_{c2} transition, a thermal hysteresis is observed down to ca. 185 K.

Discussion

Crystal Structure and the Isostructural Family of $[C(NH_2)_3]MX_3$

The anions in the crystal of $[C(NH_2)_3]HgBr_3$ consist of infinite chains formed by almost planar $HgBr_3^-$ units interconnected via two short Hg···Br(2) contacts per anion unit. The Hg atoms complete a trigonal bipyramidal coordination ($HgBr_5$) to form a single chain of $(HgBr_5)_\infty$ running along the *c* direction. In contrast to the double chain of $HgBr_5$ polyhedra in $CH_3NH_3HgBr_3$ [2], the packing of the single chain of $(HgBr_5)_\infty$ in the present compound allows to produce a space which is large enough to accommodate the larger $[C(NH_2)_3]^+$ ion.

Usually, RMX_3 (M = Cd or Hg) crystallizes in different structures; for example, the structure of $CH_3NH_3HgBr_3$ [2] is quite different from that of the Cd analogue [4]. Furthermore, as can be seen in the series of compounds $CH_3NH_3HgX_3$ (X = Cl, Br, and I), the structures of $RHgX_3$ vary also depending on the species of halogen ions [2, 8]. Then, it is notable that $[C(NH_2)_3]CdBr_3$, $[C(NH_2)_3]HgBr_3$, and $[C(NH_2)_3]HgI_3$ are isomorphous in spite of the wide variety of possible structures expected from the difference in the species of metal and halogen ions. This observation would be due to the unique character of the $[C(NH_2)_3]^+$ ion.

The Hg-Br(1) (251.0 pm) and Hg-Br(2) (257.0 pm) distances in $HgBr_3^-$ are shorter than the corresponding Cd-Br(1) (255.0 pm) and Cd-Br(2) (260.0 pm) in $CdBr_3^-$. On the other hand, the Hg···Br(2)

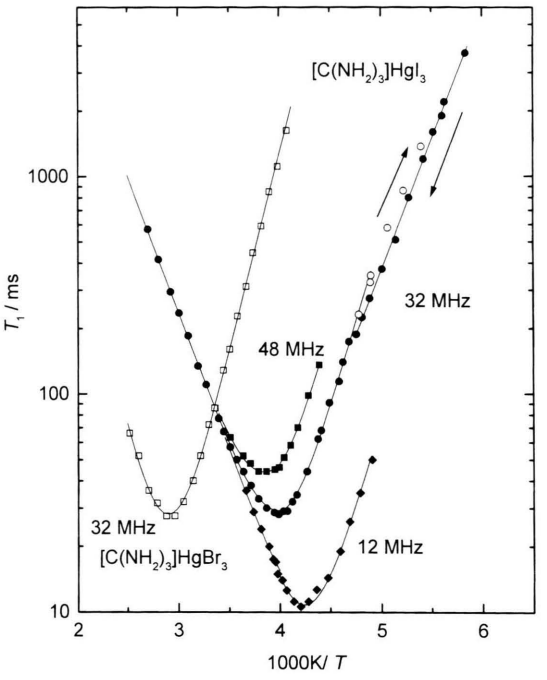

Fig. 5. Temperature dependence of ^1H NMR T_1 in $[C(NH_2)_3]HgBr_3$, □, and $[C(NH_2)_3]HgI_3$, ■: 48, ●: 32, ◆: 12 and ○: 32 MHz (for supercooled ITP). Solid lines were calculated by using (1) and (2) and the parameters given in Table 5.

bond (316.8 pm) is longer than the corresponding Cd···Br(2) bond (292.5 pm). Therefore, the $HgBr_5$ polyhedron is more distorted than that of $CdBr_5$. This is reasonable because the Cd atoms tend to make more ionic bonds with the Br atoms. The short Br···N contacts (354.9 and 357.9 pm) in $[C(NH_2)_3]HgBr_3$ are comparable to those (349.3 and 366.2pm) in the Cd analogue, for which the presence of the N-H···X hydrogen bonds has been deduced [4]. Notice that the ^{81}Br NQR line (ν_2) of the bridging Br atom of $[C(NH_2)_3]CdBr_3$ [4] shows an anomalous positive temperature dependence but the corresponding line of $[C(NH_2)_3]CdBr_3$ does not.

Molecular Motion and Phase Transition

The temperature dependence of ^1H NMR T_1 is shown in Figure 5. For the bromide, a simple V-shaped $\log T_1$ vs. $1/T$ curve was obtained. For the iodide, the T_1 minimum at 48 and 32 MHz is seen near the T_{c1} transition, and the minimum at 12 MHz is clearly in the LTP. It is well known that planar $[C(NH_2)_3]^+$ cations usually undergo C_3 reorientation in solids [9].

Table 5. Motional parameters of the C_3 reorientation of the guanidinium cations in $[C(NH_2)_3]HgBr_3$ and $[C(NH_2)_3]HgI_3$.

Compound (Phase)	C/s^{-2}	τ_0/s	$E_a/kJmol^{-1}$
$[C(NH_2)_3]HgBr_3$	5.00×10^9	1.5×10^{-14}	35.0
$[C(NH_2)_3]HgI_3$			
(RTP)	4.82×10^9	2.9×10^{-14}	24.1
(ITP)	4.90×10^9	1.8×10^{-15}	30.1
(LTP)	—	—	23.0

Judging from the observed T_1 minima, we can assign the temperature dependence of T_1 to the C_3 reorientation of the cations in both $[C(NH_2)_3]HgBr_3$ and $[C(NH_2)_3]HgI_3$. We analyzed T_1-T curves by assuming the BPP-type equation and an Arrhenius equation for the correlation time τ of the C_3 reorientation:

$$T_1^{-1} = C[\tau/(1+\omega^2\tau^2) + 4\tau/(1+4\omega^2\tau^2)] \quad (1)$$

and

$$\tau = \tau_0 \exp(E_a/RT), \quad (2)$$

where ω is an angular resonance frequency. By the least-squares calculations according to (1) and (2), the motional constant C, the correlation time at infinite temperature τ_0, and the activation energy E_a were determined. Table 5 shows these motional parameters thus obtained. As the line shapes of ^1H NMR for the iodide were not changed through both phase transitions (a motional broadening is observed below 185 K, where T_1 became longer than 1 s), the motional modes are the same in three phases.

Of the isostrucural family of $[C(NH_2)_3]CdBr_3$, $[C(NH_2)_3]HgBr_3$, and $[C(NH_2)_3]HgI_3$, only $[C(NH_2)_3]HgI_3$ undergoes phase transitions. The relatively low E_a value for the iodide indicates the ease of the occurrence of the C_3 reorientation, although the E_a has not been reported for the Cd compound. Then, the appearance of the phase transitions may be correlated to the easy occurrence of the $[C(NH_2)_3]^+$ reorientation. As seen in the above description, the short N···Br contacts in $[C(NH_2)_3]HgBr_3$ are comparable to those in the Cd analogue, for which the presence of the N-H···Br hydrogen bonds has been reported. The N-H···I interaction in the iodide would be weaker than the N-H···Br interaction in the bromide, resulting in the relatively low E_a.

The phase transition between the LTP and ITP is of first-order for the following reasons: (i) the strong

hysteresis including super-heating and (ii) the discontinuous split of the ^{127}I NQR frequencies at T_{c2}. On the other hand, the transition between the ITP and RTP seems to be of second-order as indicated by the absence of hysteresis, and the continuation of the ^{127}I NQR frequencies as well as that of ^1H T_1 at T_{c1}. The result that the ν_1 frequency is almost unchanged while the ν_2 frequency steeply increases on lowering the temperature of the ITP suggests that the HgI_5 units in the chain gradually strengthen the isolated HgI_3^- nature. A detailed discussion on these points, however, will be postponed till knowledge of the crystal structure of the ITP becomes available.

In summary, we prepared the title compounds $[C(NH_2)_3]HgBr_3$ and $[C(NH_2)_3]HgI_3$. The iodide undergoes two phase transitions at (251 ± 1) K and at (210 ± 1) K. The crystal structure of the bromide was solved at room temperature by single crystal X-ray diffraction. The room temperature phase of the iodide is isomorphous with the bromide. The temperature dependence of halogen NQR frequencies as well as ^1H NMR T_1 was measured as a function of temperature. It is suggested that the occurrence of the phase transitions in $[C(NH_2)_3]HgI_3$ is closely related to the weak H-bonding of the cations connecting the anionic chains, and hence to their large motional freedom compared with the isomorphous $[C(NH_2)_3]HgBr_3$ and $[C(NH_2)_3]CdBr_3$, which have no phase transitions.

[1] A. Ben Salah, J. W. Bats, H. Fuess, and A. Daoud, Z. Kristallogr. **164**, 259 (1983).

[2] M. Körfer, H. Fuess, J. W. Bats, and G. Klebe, Z. Anorg. Allg. Chem. **525**, 23 (1985).

[3] L. Sobczyk, R. Jakubas, and Zaleski, Polish J. Chem. **71**, 265 (1997).

[4] V. G. Krishnan, Shi-qi Dou, and Al. Weiss, Z. Naturforsch. **46a**, 1063 (1991). Crystal data: monoclinic, space group C2/*c*, *a* = 777.8(3), *b* = 1598.3(6), *c* = 746.0(3) pm, β = 110.18(1)°.

[5] MSC, 3200 Research Forest Drive. The Woodslands. TX 77381, USA (1992). Molecular Structure Corporation. TEXAN. TEXRAY Structure Analysis Package.

[6] M. C. Burla, M. Camalli, G. Cascarano, C. Giacovazzo, G. Polidori, R. Spagna, and D. Viterbo, J. Appl. Cryst. **22**, 389 (1989).

[7] H. Terao and T. Okuda, Z. Naturforsch. **45a**, 343 (1990).

[8] A. Ben Salah, J. W. Bats, R. Kalus, H. Fuess, and A. Daoud, Z. Anorg. Allg. Chem. **493**, 178 (1982).

[9] S. Gima, Y. Furukawa, and D. Nakamura, Ber. Bunsenges. Phys. Chem. **88**, 939 (1984).